

Miscible and Core–Sheath PS/PVME Fibers by Electrospinning

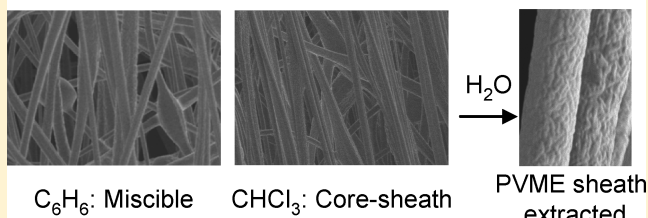
Dominic Valiquette and Christian Pellerin*

Département de chimie and Centre for Self-Assembled Chemical Structures, Université de Montréal, Montréal, QC H3C 3J7, Canada

Supporting Information

ABSTRACT: We demonstrate that miscible and phase-separated fibers of the blend between polystyrene (PS) and poly(vinyl methyl ether) (PVME) can be electrospun by appropriate selection of the solvent. Solutions in benzene allow preparing miscible fibers with composition ranging from pure PS to PS/PVME 70/30. Results indicate that the rapid solvent evaporation during electrospinning has no significant influence on the phase behavior of polymer blends when the system is miscible throughout the ternary phase diagram. On the other hand, fibers electrospun from chloroform solutions show a clear phase separation because of a closed immiscibility loop. They are nevertheless highly malleable, in contrast with the brittle films obtained by solution casting. The confinement and solvent evaporation kinetic lead to a core–sheath structure, with the interior composed of the PS-rich phase and the surface highly enriched in PVME, as opposed to microdomains in cast films. The shell can be extracted rapidly and efficiently by a 10 s treatment in water, converting the mat from fully wettable to highly hydrophobic.

Electrospinning of PS / PVME blends



INTRODUCTION

Electrospinning is probably the most common method for preparing polymeric nanofibers. In this simple and versatile technique, the application of a large electric field converts an entangled polymer solution into continuous fibers with diameters ranging from tens of nanometers to a few micrometers.^{1–4} Because of their high surface/volume ratio, electrospun fibers can find applications in textiles, filtration membranes, tissue engineering, catalysis, and nanocomposites. It is now well established that the fiber morphology (such as their diameter, their macroscopic alignment, the presence of beads, etc.) depends on solution parameters such as the solution concentration and the nature of the solvent as well as on processing conditions such as the amplitude of the electric field and the type of collector used.^{1–4}

A growing fraction of electrospinning studies involve polymer composites or mixtures. In many cases, a flexible polymer is used as a supporting matrix for systems that could not be electrospun by themselves due to a lack of entanglement in solution, such as nanoparticles, oligomers, and drugs.^{5–8} The matrix can often be later removed by selective dissolution or thermal degradation. The electrospinning of blends of two polymers is also important since it allows forming fibers from polymers with a limited solubility or that are too rigid to form a well-entangled network, obtaining porous nanofibers by selective extraction of one of the polymers or more generally preparing fibers with tailored properties at lower cost.^{9–12} A few polymer couples can produce miscible blends because of their specific interactions but their electrospinning has been rarely reported.¹¹ In contrast, the vast majority of polymers form immiscible blends because of their low mixing entropy. Their fibers are therefore phase separated with a morphology that depends on the molecular weight of the

polymers, their surface energy, the blend composition, and the solvent selection.^{12–15} The most commonly observed morphologies are (i) two cocontinuous phases, (ii) nanodomains of one phase dispersed in a matrix of the other, and (iii) a core–sheath structure.

The ultrarapid solvent evaporation that occurs during electrospinning adds a key kinetic component to the thermodynamic interactions that normally define the miscibility of a blend. The formation of unusual or metastable crystalline structures has already been reported for several homopolymers.^{16–18} We have recently observed the influence of kinetics during the electrospinning of mixtures of poly(ethylene oxide) with various small molecules such as urea, thiourea, and hydroquinone.^{19–21} Fibers consisted of a pure supramolecular complex as opposed to the inhomogeneous mixtures obtained by a slower solvent casting process. An interesting kinetic effect has also been reported recently for the electrospinning of the polylactide/polyaniline blend for which miscible fibers were obtained even if the slowly cast films were immiscible.²²

Blends of polystyrene (PS) with poly(vinyl methyl ether) (PVME) constitute a system of choice to study the interplay between the thermodynamic aspects of polymer mixing and the kinetic nature of the electrospinning process. It is well-known that miscible and ductile PS/PVME films can be obtained by slow casting from solutions in solvents such as benzene or toluene.^{23–25} In sharp contrast, films cast from chloroform or trichloroethylene solutions present a marked phase separation at the micrometer scale which results in films with mediocre

Received: September 13, 2010

Revised: February 4, 2011

Published: March 30, 2011

mechanical properties.²³ In this paper, we have explored the electrospinning of PS/PVME blends using benzene and chloroform as model solvents leading to miscible and phase-separated films, respectively. Continuous and malleable fibers could be obtained from both solvents, in contrast with our expectation. The solvent selection nevertheless has a large impact on the structure and physical properties of the PS/PVME fibers.

EXPERIMENTAL SECTION

Atactic PS (Scientific Polymer Products) with an average molecular weight (M_w) of 210 000 g/mol, tetrabutylammonium bromide (TBAB, Acros Organics), benzene, and chloroform (Fisher Scientific) were used as received. Atactic PVME (Scientific Polymer Products) with an M_w of 90 000 g/mol was received in a toluene solution. Most toluene was first removed by evaporation under vacuum at moderate temperature to prevent oxidation. The polymer was then dissolved in benzene and evaporated under vacuum at 50 °C for 4 days to remove traces of solvent, as confirmed by infrared spectroscopy and the observation of a constant glass transition temperature (T_g).

Solutions were prepared by dissolving a total concentration of 25% (w/v) of the polymers in either chloroform or benzene. Throughout this paper, the blends will be labeled according to their PS/PVME mass ratio, such that a 70/30 mixture contains 70% of PS and 30% of PVME. A concentration of 3.88×10^{-4} mol/L of TBAB was added to solutions in benzene to improve their electrospinnability. This corresponds to 0.5% (w/w) of the dry polymer mass. Solutions were agitated for at least 4 h before being introduced in a 5 mL glass syringe equipped with a 0.41 mm flat-ended needle. A voltage of 18 kV was applied on the needle using a CZE 100R high-voltage power supply (Spellman High Voltage Electronics) while a -2 kV potential was imposed on the counter electrode located 15 cm from the needle. The flow rate was adjusted to 0.9 mL/h using a PHD 2000 syringe pump (Harvard Apparatus). Thin films with various PS/PVME compositions were also prepared to provide comparison or calibration values for the characterization of the electrospun fibers. Films were cast from 3% (w/v) solutions in benzene or chloroform and were dried under vacuum at temperatures up to 10 °C above T_g to remove traces of solvent.

Scanning electron microscopy (SEM) images were recorded using a Hitachi J1400 microscope. A thin layer of gold was deposited on the sample prior to observation. Differential scanning calorimetry (DSC) measurements were carried out with a 10 °C/min heating rate using a TA Instruments Q2000 calorimeter calibrated with ultrapure indium. Infrared spectra with a 4 cm^{-1} resolution were recorded using a Tensor 27 FT-IR spectrometer (Bruker Optics) equipped with a liquid nitrogen-cooled HgCdTe detector and a GoldenGate (Specac) diamond attenuated total reflection accessory. Contact angle measurements were conducted with the sessile drop method using an FTA200 dynamic contact angle analyzer (First Ten Angstroms). 5 μL droplets of Milli-Q quality water were used as the probe liquid, and 10 separate measurements were averaged for each fiber mat or film.

RESULTS AND DISCUSSION

Benzene and chloroform were selected as solvents because they impart drastically different structures to PS/PVME films after a slow solvent casting.²³ Electrospun fibers of pure PS can be produced rather easily when using concentrated solutions in chloroform. In contrast, solutions in benzene simply dripped off the tip of the needle at voltages as high as 25 kV, which is explained by the low dielectric constant of benzene (2.28) as compared to chloroform (4.81). The other solvents known to form miscible films, toluene, xylene, and tetrachloroethylene are not better options because they possess a similar dielectric

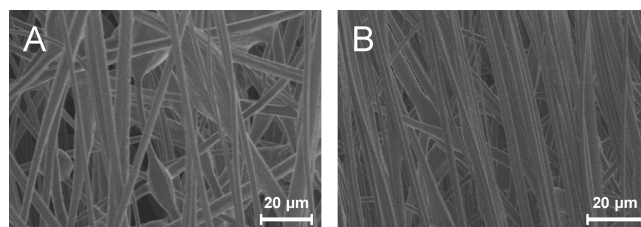


Figure 1. SEM micrographs of PS/PVME 70/30 fibers electrospun from (A) benzene and (B) chloroform.

constant in addition to a higher boiling point. Tetrabutylammonium chloride (TBAB), an organic salt highly soluble in benzene, was therefore added to increase the conductivity.^{26,27} Beaded fibers could be produced in good yield with a TBAB concentration of at least 0.5% w/w of polymer. Such beaded fibers are often observed during electrospinning because fluid instabilities favor the capillary breakup of the jet into droplets until it solidifies.^{28,29} In the case of unentangled solutions, complete breakup of the jet leads to electrospray rather than electrospinning. The number of beads per fiber decreased for higher TBAB concentrations because of charge repulsion and beadless fibers could be obtained with at least 2% of TBAB. The minimum concentration of 0.5% was nevertheless used throughout this study to limit its potential impact on the structure of the blend.

Figure 1 shows typical SEM images obtained for PS/PVME 70/30 fibers electrospun from benzene and chloroform. The fibers are continuous and present a bead-on-string morphology. Several fibers present an extended longitudinal wrinkle that can be attributed to a faster solvent evaporation at the surface of the electrified jet.³⁰ Their average diameter is relatively large (2–3 μm), which is not surprising considering the high polymer concentration required to create a well-entangled network in solution. The morphology and diameter distribution are in fact quite similar for all fibers, irrespective of the composition and solvent used. Attempts to electrospin blends with 60% or less of PS from benzene solutions were unsuccessful since the fibers quickly broke into droplets on the collector. Large (several micrometers) and sticky fibers could be obtained from chloroform solutions for the 60/40 and 50/50 blends, even if the solutions were cloudy and therefore already in the two-phase region of the ternary phase diagram.

While this may appear trivial, the production of continuous fibers from chloroform solutions is an unexpected result. These fibers are malleable and can be kept freestanding on a frame for months without showing a clear loss of mechanical integrity. This is completely at odds with the waxy films that are obtained when solvent casting the same solutions. Infrared spectra were recorded to verify if the fibers electrospun from chloroform solutions were truly composed of a PS/PVME blend or if PS was preferentially spun. Figure 2 shows that very similar spectra are obtained for 70/30 fibers spun from benzene and chloroform. The relative absorbance of the 2850 and 2820 cm^{-1} bands, which are due to CH_2 and CH_3 stretching modes in PS and PVME, respectively, clearly indicates that the composition in the fibers is identical to that in the starting solution.

DSC measurements were conducted to determine if the phase behavior of the fibers is different from that of slowly evaporated films. Figure 3 shows that the fibers electrospun from benzene possess a single T_g that evolves with composition, indicating that

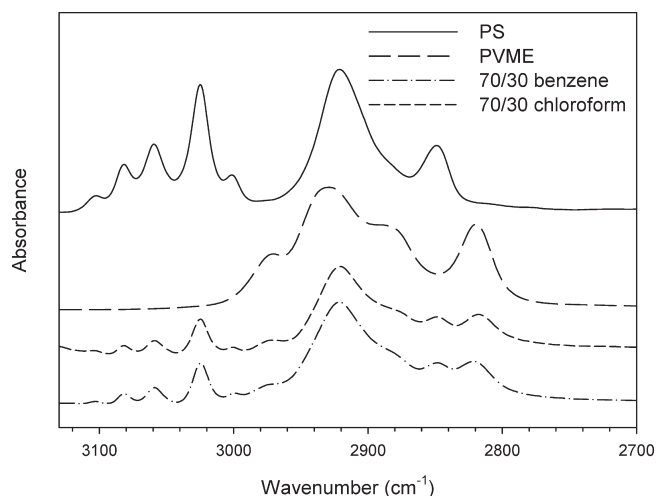


Figure 2. Infrared spectra of the pure polymers and of PS/PVME 70/30 fibers electrospun from benzene and chloroform.

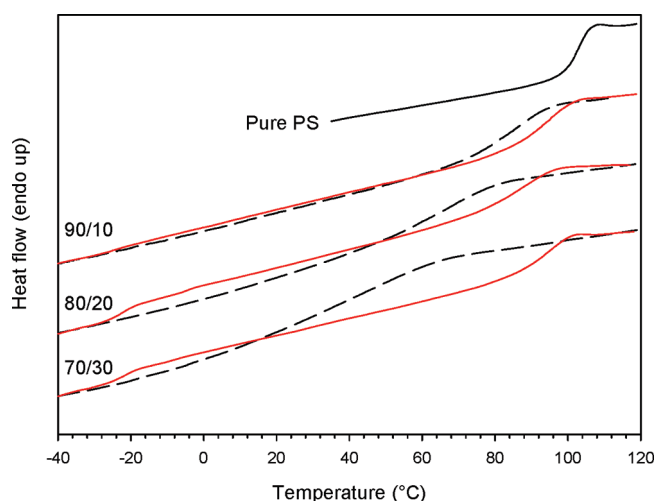


Figure 3. DSC thermograms showing the miscibility of fibers electrospun from benzene (dashed lines) and the phase separation of fibers electrospun from chloroform (full lines) for various PS/PVME mixtures.

miscibility is preserved in these samples. An accurate determination of T_g is difficult because the transition region is very broad, more than 50 °C in the 70/30 blend. Nevertheless, Figure 4 shows that its evolution with composition is very similar in the fibers and in solvent-cast miscible films. The broadening of the glass transition region is a common phenomenon for blends consisting of polymers with very different T_g s, leading to thermorheological complexity. It has been explained by some authors by the existence of dynamic heterogeneities (or concentration fluctuations) at the nanometer scale.^{24,31,32} In contrast, Lodge and McLeish have proposed a model in which the T_g broadening is explained solely by considering the effect of self-concentration on the effective T_g of each component of the blend.^{24,33} Most recently, Kumar et al. have combined both approaches to consider intramolecular and intermolecular concentration fluctuations.³⁴ They found excellent agreement between the model and dielectric spectroscopy results for PS/PVME blends. It should be noted that the transition breadth is identical for the fibers electrospun from benzene and for films

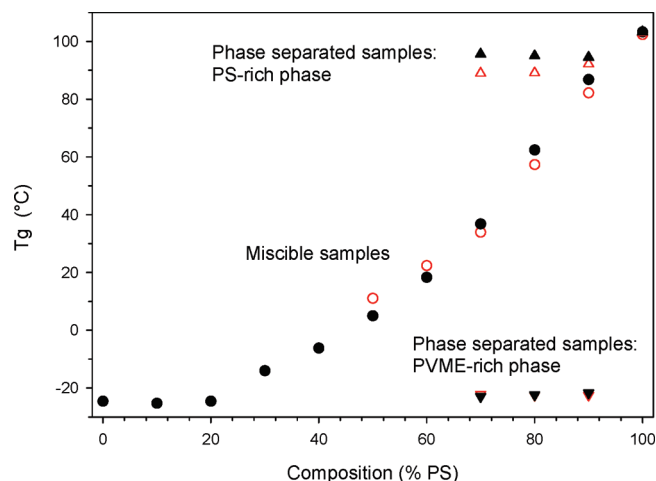


Figure 4. Evolution of T_g in PS/PVME electrospun fibers (open symbols) and slowly cast films (filled symbols) with blend composition. Miscible films and fibers (circles) were obtained from benzene solutions and present a single T_g . Phase-separated films and fibers were obtained from chloroform solutions and present two T_g s for the PS-rich phase (upward triangles) and PVME-rich phase (downward triangles).

cast from the same solvent, indicating that the fibers are at least as miscible as the films. Combined with the results of Figure 4, it can be concluded that the electrospinning process has no significant influence on the phase behavior of polymer blends when the thermodynamics of mixing favor miscibility throughout the ternary phase diagram. The difficulty in obtaining fibers with 60% PS or less comes from their low T_g which is at or below room temperature. The mobility of the polymer chains in the rubbery state is relatively high even if the solvent has completely evaporated. Fibers can fleetingly be formed but they eventually break into droplets to lower their surface energy.

In contrast with the miscible fibers produced from benzene solutions, the thermograms of Figure 3 clearly show two distinct T_g s for fibers electrospun from chloroform. This proves unambiguously their phase separation into PS-rich and PVME-rich phases. Figure 4 compares the evolution of the T_g s for both phases in the fibers and in films obtained by casting from chloroform. The composition of the phases can then be estimated by comparing their T_g with those of miscible films. The T_g of the rubbery PVME-rich phase is almost constant at -22 ± 1 °C for all films and fibers, very close to that of pure PVME (-24 °C). This phase contains $\sim 80\%$ of PVME and only 20% of PS, strongly departing from the average composition of the blend. The T_g of the PS-rich phase in the films is almost constant at 95 °C, and it is only slightly lower in the fibers, ranging from 92 °C in the 90/10 blend to 89 °C in the 70/30 blend. The composition of these PS-rich phases varies in a narrow range between 95/5 and 93/7. Of course, the relative quantity of PS-rich and PVME-rich phases evolves with the global composition of the mixture, as can be noted in Figure 3 by observing the height of the heat capacity jumps at each T_g .

These results indicate that an extensive phase separation occurs in the fibers electrospun from chloroform. Under thermodynamic equilibrium conditions, PS and PVME form miscible samples because of the favorable mixing entropy and of enthalpic interactions between the phenyl rings and the methoxy groups²⁵ that lead to a small but negative interaction parameter.³⁵ This behavior is observed for films and fibers prepared from benzene.

The phase separation observed when casting or electrospinning samples from chloroform originates from the stronger affinity of chloroform for PVME than for PS. Chloroform is a good solvent for both polymers, but its interaction parameter with PS and PVME is 0.13 and -0.92 , respectively, so that it is a much better solvent for PVME.²⁵ The phase diagram of the PS/PVME/chloroform ternary system shows that solutions are miscible at low concentration but that a closed region of immiscibility exists for more concentrated solutions.³⁶ As a consequence, separation into PS-rich and PVME-rich (liquid) phases occurs during solvent evaporation. In very highly concentrated solutions, the whole system should in principle return to a completely miscible state, since the PS/PVME blend itself (without chloroform) is thermodynamically miscible. In practice, the DSC scans of Figure 3 clearly show that the phase-separated structure is preserved in fibers obtained from chloroform. The phase separation is therefore metastable and kinetically frozen by the very high viscosity when the solvent fraction becomes small.

The similarity of the composition of the phases observed in Figure 4 for phase-separated films and fibers, for all global compositions, suggests that the liquid–liquid phase separation during solvent evaporation occurs by a mechanism of nucleation and growth rather than through a spinodal decomposition. The malleability of the fibers, as opposed to the waxy nature of the films, must therefore originate from the morphology of the phases and not their local composition. Slow casting leads to the formation of micrometer-sized domains throughout the film, a morphology that is incompatible with the continuous fibers obtained in this work since their diameter is in the range of $\sim 2\text{--}3\text{ }\mu\text{m}$. Electrospinning would result from such large-amplitude phase separation since the connectivity of the fibers would be broken during the phase separation process. On the other hand, miscible fibers could have been obtained if the solvent evaporation rate had occurred very fast as compared to the kinetics of phase separation in the closed immiscibility loop of the ternary phase diagram. Such “quenching” of the solution in a state of miscibility (assuming that the starting solution is miscible) likely explains the results obtained by Picciani et al., who observed miscible polylactide/polyaniline fibers even if slow casting led to phase-separated films.²² This scenario is obviously not observed here, so the structure in the fibers must result from the competition between solvent evaporation and the kinetics of phase separation in the concentrated solution.

Two scenarios are most plausible for the structure in the fibers. In the first, domains of the minor phase could be randomly distributed through the fiber, as in bulk films, but their average size would be much smaller than in films due to a shorter phase separation time (as mentioned above, fiber breakage would have occurred with micrometer-sized domains). A continuous matrix of the PS-rich phase could then maintain the mechanical integrity of the fibers as it does in miscible fibers. The second possibility is a core–sheath structure, in which the PVME-rich phase would be located preferentially at the surface. Again, a PS-rich matrix could maintain mechanical integrity of the fibers. A PS-rich sheath is unlikely since (1) PVME has a lower surface energy than PS so that it should segregate to the surface, as previously observed in ultrathin films,^{38,39} and (2) PVME is more soluble in chloroform than PS, as described above, so that a PS core should solidify first. A third case, the formation of a cocontinuous morphology, is less likely considering that mass fraction of the PVME-rich phase can be estimated to 30% and only 5% in the 70/30 and 90/10 blends, respectively.

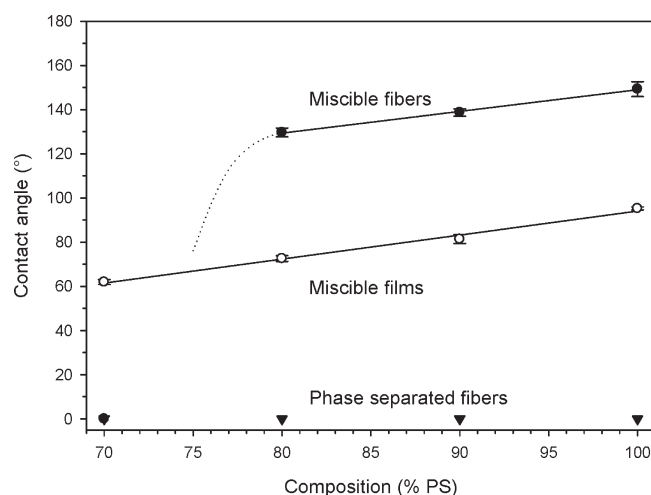


Figure 5. Evolution of the water contact angle with blend composition for miscible and immiscible PS/PVME fibers electrospun from benzene and chloroform, respectively. The contact angles for miscible films slowly cast from benzene are shown for comparison.

To investigate which model best describes the fibers morphology, water contact angle (WCA) measurements were carried on the miscible and phase-separated fibers and compared with results obtained for miscible films. Figure 5 shows that the WCA of miscible films decreases linearly from 95° for pure PS to 62° for the 70/30 blend due to the presence of the hydrophilic PVME. Much higher WCA values were measured for the miscible fibers as compared to their equivalent film. This $\sim 55^\circ$ increase in WCA is well explained by the Cassie–Baxter model, which takes into account the presence of air gaps between individual fibers that limit the droplet penetration in a porous mat as compared to a continuous film of the same material.³⁷ In our case, the fibers only constitute $\sim 22\%$ of the interface, leading to much higher WCA. In particular, an average WCA of 149° , close to superhydrophobicity, was obtained for mats of pure PS fibers. In contrast with the PS-rich miscible fibers, the water droplets completely penetrated the mat when the fibers contained at least 30% of PVME, leading to an apparent WCA of 0° . Values of 0° were also found for all the phase-separated fibers, thereby indicating the presence of at least 30% of PVME on their surface, even for the 90/10 blend. These results strongly support the core–sheath model in which the surface of the phase-separated fibers is strongly enriched in PVME while its core is composed of the PS-rich matrix.

In order to provide support to the core–sheath hypothesis, a selective extraction of PVME was attempted by immersing the miscible and phase-separated PS/PVME 70/30 fibers in cold water ($1\text{--}2\text{ }^\circ\text{C}$), a nonsolvent for PS. Infrared spectroscopy was used to quantify the composition of the fibers as a function of immersion time by following the ratio of the PVME and PS bands at 2820 and 2850 cm^{-1} , respectively. For the miscible fibers, Figure 6 shows that the PS fraction increases only modestly from 70 to $74 \pm 2\%$ after 1 min of immersion. This is not surprising since most PVME chains are well entangled with the hydrophobic PS chains. The partial extraction could be explained by a small fraction of poorly entangled chains at the surface and by a surface enrichment in PVME. Previous studies on ultrathin films of miscible PS/PVME blends have reported such effect due to the lower surface energy of PVME.^{38,39} In sharp contrast with the miscible fibers, the PS fraction in the immiscible fibers increased

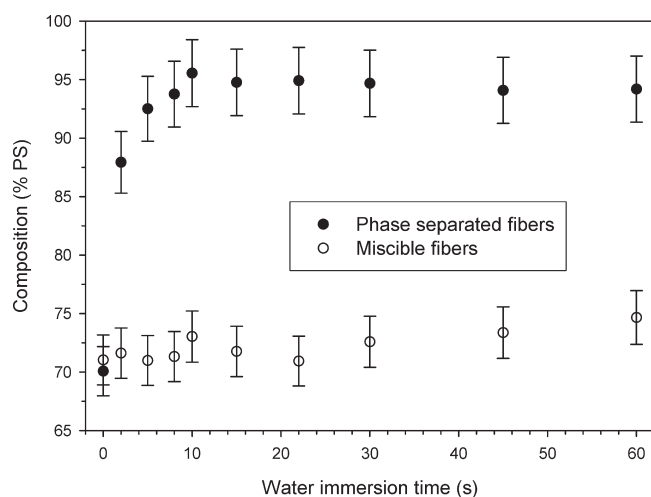


Figure 6. Evolution of the composition of miscible and immiscible PS/PVME fibers as a function of the immersion time in water. Compositions were determined by infrared spectroscopy.

abruptly from 70% to $94 \pm 2\%$ in 10 s. The composition remained constant for longer immersion times, including after 5 days of treatment. To emphasize the speed of the process, 68% of the PVME initially present in the fibers was extracted within the first 2 s, and 85% was removed after 10 s. The efficiency of the extraction confirms that the PVME chains are essentially located at the surface, in agreement with the core–sheath model. The immiscible fibers are therefore composed of a PS-rich matrix covered by a PVME-rich surface layer. If present, domains distributed within the hydrophobic matrix should be mostly unaffected by the extraction process since water can hardly penetrate the hydrophobic PS-rich phase. The number of these putative domains must be small because the final composition of the extracted fiber is very close (identical within error) to that of the PS-rich phase before treatment.

Water contact angle measurements provide further support for the removal of a PVME-rich surface layer upon immersion in water. Indeed, the WCA increased dramatically from 0° for the starting mat to 133° after water extraction. Such a conversion from a fully wettable to a very highly hydrophobic mat could lead to application as a very cheap indicator of water exposure for sensitive materials. In fact, an even larger WCA value of 143° could have been expected by interpolating the data of Figure 5 to the final composition (94/6) after extraction. The lower observed WCA is likely due to a slight compaction of the mat upon exposure to water that reduces the fraction of air gaps and therefore the WCA in the Cassie–Baxter model. Indeed, a similar reduction ($\sim 13^\circ$) was observed after immersing mats of pure PS in water even if they are completely insoluble. A better adhesion of the mat to its substrate could therefore provide an even more extreme change in surface properties.

Finally, SEM pictures recorded before and after a 45 s immersion (Figure 7) indicate that the surface of the initial fibers is relatively smooth, but it becomes very rugged after treatment. The deep or interconnected pores that would have been expected for a cocontinuous system are not observed. The roughness of the treated fibers suggests that the interface between the PS-rich core and PVME-rich surface is not smooth. The core is more than 70°C below its T_g and is water-insoluble so it probably maintains the shape of the interface that was created by the liquid–liquid phase separation during chloroform evaporation. Since the PVME-rich phase is more than 40°C

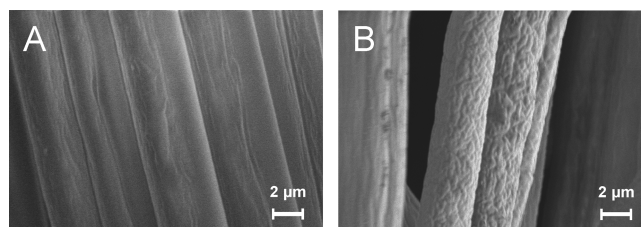


Figure 7. SEM micrographs of PS/PVME 70/30 fibers electrospun from chloroform (A) before and (B) after a 45 s immersion in water.

above its T_g at room temperature, it can easily flow to create the relatively smooth outer surface observed for the starting fibers in order to reduce the surface energy. A crude calculation indicates that the thickness of the PVME-rich sheath (assuming it is continuous) should be on the order of several tens of nanometers if a complete phase separation had occurred. It is not possible to study such a small decrease because of the large diameter of the fibers and their broad distribution.

It is interesting to note that a core–sheath structure easily explains the observation of sticky fibers for the 60/40 and 50/50 blends electrospun from chloroform since their surface should be covered by a relatively thick viscous layer with a T_g of -22°C . It also explains the ease of producing durable phase-separated fibers at these compositions for which miscible fibers quickly broke into droplets. Indeed, the high T_g of the PS-rich core drastically limits the mobility of the chains and allows maintaining the mechanical integrity of the fibers. In contrast, the whole fiber is at or above its T_g for the miscible system, so that a rapid breakup into droplet is possible during or after electrospinning.

CONCLUSION

The electrospinning of blends of PS with PVME can produce miscible or phase-separated fibers by a proper selection of the solvent. Both types of fibers are malleable and can be handled for extended periods of time, which was an unexpected result for the phase-separated fibers. The miscible fibers are characterized by a single glass transition that is similar in position and breadth to that observed in miscible solvent-cast films of the same composition, indicating that the electrospinning process does not affect the structure of miscible blends. In contrast, the phase-separated fibers present a core–sheath morphology, as opposed to the microdomains normally observed in PS/PVME films cast from chloroform. The core is formed by the PS-rich phase while the sheath contains $\sim 80\%$ of PVME. This sheath can be completely extracted by immersion in water in as little as 10 s. This process leads to a drastic change in surface properties from completely wettable to strongly hydrophobic (contact angle of 133°).

ASSOCIATED CONTENT

S Supporting Information. Additional TEM and SEM images are provided to support the core–sheath model for the phase-separated fibers. This material is available free of charge via the Internet at <http://pubs.acs.org>.

AUTHOR INFORMATION

Corresponding Author

*Tel (514) 340-5762; fax (514) 340-5290; e-mail c.pellerin@umontreal.ca.

■ ACKNOWLEDGMENT

The authors thank the Natural Sciences and Engineering Research Council of Canada (NSERC) for supporting this work and Marie Richard-Lacroix for conducting complementary experiments, Damien Mauran for his assistance for the DSC and IR studies, and Sylvia Francis-Zalzal and Prof. Antonio Nanci for performing additional SEM and TEM experiments.

■ REFERENCES

- (1) Burger, C.; Hsiao, B. S.; Chu, B. *Annu. Rev. Mater. Res.* **2006**, 36, 333.
- (2) Greiner, A.; Wendorff, J. H. *Angew. Chem., Int. Ed.* **2007**, 46, 5670.
- (3) Doshi, J.; Reneker, D. H. *J. Electrostat.* **1995**, 35, 151.
- (4) Dzenis, Y. *Science* **2004**, 304, 1917.
- (5) Hu, W.; Huang, Z. M.; Liu, X. Y. *Nanotechnology* **2010**, 21, 315104.
- (6) Zhang, Z. Y.; Li, X. H.; Wang, C. H.; Wei, L. M.; Liu, Y. C.; Shao, C. L. *J. Phys. Chem. C* **2009**, 113, 19397.
- (7) Salalha, W.; Dror, Y.; Khalfin, R. L.; Cohen, Y.; Yarin, A. L.; Zussman, E. *Langmuir* **2004**, 20, 9852.
- (8) Xiang, C. H.; Joo, Y. L.; Frey, M. W. *J. Biobased Mater. Bioenergy* **2009**, 3, 147.
- (9) Bianco, A.; Bertarelli, C.; Frisk, S.; Rabolt, J. F.; Gallazzi, M. C.; Zerbi, G. *Synth. Met.* **2007**, 157, 276.
- (10) Babel, A.; Li, D.; Xia, Y. N.; Jenekhe, S. A. *Macromolecules* **2005**, 38, 4705.
- (11) Allakhverdiev, K. R.; Lovera, D.; Altstadt, V.; Schreier, P.; Kador, L. *Rev. Adv. Mater. Sci.* **2009**, 20, 77.
- (12) Bognitzki, M.; Frese, T.; Steinhart, M.; Greiner, A.; Wendorff, J. H.; Schaper, A.; Hellwig, M. *Polym. Eng. Sci.* **2001**, 41, 982.
- (13) Chen, M. L.; Dong, M. D.; Havelund, R.; Regina, V. R.; Meyer, R. L.; Besenbacher, F.; Kingshott, P. *Chem. Mater.* **2010**, 22, 4214.
- (14) Park, K. E.; Kang, H. K.; Lee, S. J.; Min, B. M.; Park, W. H. *Biomacromolecules* **2006**, 7, 635.
- (15) Wei, M.; Kang, B. W.; Sung, C. M.; Mead, J. *Macromol. Mater. Eng.* **2006**, 291, 1307.
- (16) Yee, W. A.; Kotaki, M.; Liu, Y.; Lu, X. H. *Polymer* **2007**, 48, 512.
- (17) Stephens, J. S.; Chase, D. B.; Rabolt, J. F. *Macromolecules* **2004**, 37, 877.
- (18) Lee, K. H.; Snively, C. M.; Givens, S.; Chase, D. B. *Macromolecules* **2007**, 40, 2590.
- (19) Antaya, H.; Richard-Lacroix, M.; Pellerin, C. *Macromolecules* **2010**, 43, 4986.
- (20) Liu, Y.; Antaya, H.; Pellerin, C. *J. Phys. Chem. B* **2010**, 114, 2373.
- (21) Liu, Y.; Antaya, H.; Pellerin, C. *J. Polym. Sci., Part B: Polym. Phys.* **2008**, 46, 1903.
- (22) Picciani, P. H. S.; Medeiros, E. S.; Pan, Z.; Wood, D. F.; Orts, W. J.; Mattoso, L. H. C.; Soares, B. G. *Macromol. Mater. Eng.* **2010**, 295, 618.
- (23) Bank, M.; Leffingwell, J.; Thies, C. *Macromolecules* **1971**, 4, 44.
- (24) Pellerin, C.; Pelletier, I.; Pézolet, M.; Prud'homme, R. E. *Macromolecules* **2003**, 36, 153.
- (25) Djordjevic, M. B.; Porter, R. S. *Polym. Eng. Sci.* **1982**, 22, 1109.
- (26) Givens, S. R.; Gardner, K. H.; Rabolt, J. F.; Chase, D. B. *Macromolecules* **2007**, 40, 608.
- (27) Honda, T.; Sasada, T.; Sakamoto, T. *Jpn. J. Appl. Phys.* **1979**, 18, 1031.
- (28) Fong, H.; Chun, I.; Reneker, D. H. *Polymer* **1999**, 40, 4585.
- (29) Rutledge, G. C.; Fridrikh, S. V. *Adv. Drug Delivery Rev.* **2007**, 59, 1384.
- (30) Koombhongse, S.; Liu, W. X.; Reneker, D. H. *J. Polym. Sci., Part B: Polym. Phys.* **2001**, 39, 2598.
- (31) Zetsche, A.; Fischer, E. W. *Acta Polym.* **1994**, 45, 168.
- (32) Pathak, J. A.; Colby, R. H.; Floudas, G.; Jérôme, R. *Macromolecules* **1999**, 32, 2553.
- (33) Lodge, T. P.; McLeish, T. C. B. *Macromolecules* **2000**, 33, 5278.
- (34) Shenogin, S.; Kant, R.; Colby, R. H.; Kumar, S. K. *Macromolecules* **2007**, 40, 5767.
- (35) Han, C. C.; Bauer, B. J.; Clark, J. C.; Muroga, Y.; Matsushita, Y.; Okada, M.; Tran-cong, Q.; Chang, T.; Sanchez, I. C. *Polymer* **1988**, 29, 2002.
- (36) Robard, A.; Patterson, D.; Delmas, G. *Macromolecules* **1977**, 10, 706.
- (37) Cassie, A. B. D.; Baxter, S. *Trans. Faraday Soc.* **1944**, 40, 546.
- (38) Bhatia, Q. S.; Pan, D. H.; Koberstein, J. T. *Macromolecules* **1988**, 21, 2166.
- (39) Lee, S. M.; Sung, C. S. P. *Macromolecules* **2001**, 34, 599.